Cover Letter

This manuscript has posted as a preprint to facilitate academic exchange. The underlying technical methodology described herein is protected by intellectual property rights. We have officially filed a Chinese patent application (App. No. CN202511140743.3A) and a corresponding PCT international application (App. No. PCT/CN2026/112498).

Legal Notice on Novelty: This disclosure is made after the filing dates of the aforementioned applications. Consistent with 35 U.S.C. § 102(b)(1) and Article 24 of the Chinese Patent Law, this preprint publication serves as a non-prejudicial disclosure and does not affect the novelty or validity of the pending patent claims.

Open Access Scope: Patent protection strictly covers the technical implementation methodologies (including specific algorithms and system structures). All theoretical frameworks, empirical data analysis, and economic interpretations presented in this work remain open for academic review for the purpose of facilitating the development of the academic field. The supporting data and material is available confidentially upon request.

Intellectual Property and Patent Declaration: We hereby declare that the core methodologies, algorithmic architectures and frameworks presented in this white paper are protected by international intellectual property laws. A Patent Cooperation Treaty (PCT) international patent application has been officially filed (PCT Application No.: PCT/CN2026/112498), claiming priority to the Chinese national patent application (Application No.: CN202511140743.3A, filed on August 14, 2025). All rights regarding the commercial implementation, replication, and derivative works of the proposed systems are strictly reserved by the authors and their affiliated institution.

Thermodynamic Framework for VIX Microstructure Analysis for Systemic Risk Management: Entropy, Enthalpy, and Gibbs Free Energy

Huzi Sun, PhD[1]*

Affiliations:

[1] Sun Research & Strategy, LLC - Polyexponential.ai; New York, USA.

* Corresponding author. E-mail address: admin@polyexponentialai.com.

Abstract: This paper introduces a novel thermodynamic framework for analyzing the VIX microstructure, treating it as a thermodynamic system. We define entropy, enthalpy, and Gibbs free energy for the VIX microstructure and develop corresponding empirical measures. Our analysis reveals that the thermodynamic state variables provide valuable insights into market stability and systemic risk. The proposed framework offers a new perspective for understanding market dynamics and predicting critical transitions. Traditional volatility analytics rely heavily on discrete spot VIX thresholds or binary contango/backwardation heuristics. This paper presents a non-equilibrium classical thermodynamic state-function formulation of VIX microstructure, augmented by kinetic transport theory. By defining a normalized probability distribution, we construct a continuous entropy $S(t)$, an enthalpy $H(t)$ incorporating volatility-of-volatility (VVIX) pressure, an effective temperature $T_{eff}(t)$, and a composite Gibbs free energy potential $G(t) = H(t) - T_{eff}(t)S(t)$. Furthermore, we integrate kinetic transport concepts—specifically collision intensity and market viscosity $\eta = \frac{|T_{VVIX}|}{Kinetic}$ to model pre-crisis liquidity freezes. Empirical validation reveals that $G(t)$ exhibits an informational signal governed by the Shock Kinematics Hypothesis.

JEL Classification: C00; C60; C80; D80; G14

Keywords: Systemic risk management, Thermodynamic system, VIX microstructure, Global asset management

Introduction

The VIX index, often referred to as the "fear index," measures the market's expectation of 30-day forward-looking volatility. The VIX microstructure, which represents the relationship between VIX futures, provides crucial information about market expectations. Traditional financial models often fail to capture the complex dynamics and systemic risks embedded in the VIX microstructure.

Recent advances in econophysics have shown promise in applying physical concepts to financial markets.[5] However, a comprehensive thermodynamic framework specifically tailored for the VIX microstructure remains underexplored. This paper fills this gap by developing a thermodynamic model that quantifies market stability and systemic risk through entropy, enthalpy, and Gibbs free energy. This work's contribution is to replace this binary, qualitative distinction with a continuous, physically-motivated state-variable system borrowed from equilibrium thermodynamics — entropy, enthalpy, and Gibbs free energy — computed directly from VIX microstructure and the VIX-of-VIX index (VVIX).

What is genuinely new in this work's construction, separating it from both (a) classical VIX-threshold heuristics and (b) prior econophysics work that has generally focused on the statistical properties of return distributions rather than on a full state-function description of the volatility microstructure itself. Rather than modeling the cross-section of asset returns or a single volatility series, it constructs a complete thermodynamic state-function system (S,H, T_{eff} ,G) specifically for the volatility microstructure, and proposes a single scalar potential (G) intended to function as a real-time systemic-stability gauge.

1. Theoretical Framework and Thermodynamic Reformulation

1.1 Probability Normalization and Entropy

Rather than treating the VIX microstructure as a simple spread, the framework maps the vector of VIX microstructure $F(t,T)$ across maturities $T \in \{T_1, T_2, \ldots, T_N\}$ into a discrete probability distribution $P(T)$:

$$P(T) = \frac{F(t,T)}{\sum_T F\,(t,T)}$$

Using $P(T)$, the VIX microstructure entropy $S(t)$ is defined as:

$$S(t) = -k \sum_T P\,(T) \ln P\,(T)$$

where k is a scaling constant. Under this formulation, $S(t)$ reaches its mathematical maximum when the microstructure is perfectly flat (equal price distribution across all space). Conversely, when market stress severely distorted the microstructure, concentration of $P(T)$ causing $S(t)$ to plummet toward a local minimum. Thus, local entropy minima (S_{min}) directly mark peaks in short-term market panic, reformulating stress intensity as a continuous information-theoretic concentration index.

1.2 Enthalpy and Second-Order Volatility Pressure

To capture the total energy state of the volatility complex, the model augments spot VIX with a pressure term derived from the VIX-of-VIX index ($VVIX$). Enthalpy $H(t)$ is formulated as:

$$H(t) = VIX_{spot}(t) + \alpha \cdot (VVIX(t) - VVIX_{mean})$$

where α is a scaling coefficient and $VVIX_{mean}$ denotes the long-term baseline. Here, $VIX_{spot}(t)$ acts as the internal energy / kinetic core $U(t)$, while the $VVIX$ term acts as thermodynamic pressure. Two market environments with identical spot VIX levels are assigned fundamentally different energy profiles if their underlying vol-of-vol ($VVIX$) regimes diverge, allowing second-order uncertainty to directly shift the system's thermodynamic state.

This work's innovation at the variable-construction level include several aspects. Firstly, it fuses the level of implied volatility (VIX) with a pressure term drawn from the volatility-of-volatility index (VVIX), so that two moments with identical VIX levels but different VVIX regimes are assigned different total "energy." Secondly, it's the dynamic α scaling coefficient. Rather than imposing fixed weights on α scaling coefficient, we let the data determine their relative contribution. At each time t, the α scaling coefficient is set to its rolling-variance share:

$$H = \alpha(t) \cdot U + (1 - \alpha(t)) \cdot P, \text{ where } \alpha(t) = \sigma U(t)/(\sigma U(t) + \sigma P(t)).$$

where $\sigma U(t)$ and $\sigma P(t)$ are the rolling standard deviations, using the decay of the autocorrelation of $U(VIX)$ and $P(VVIX)$ to determine its memory length, we are using the larger decay value, i.e. the longer memory, for the rolling window.

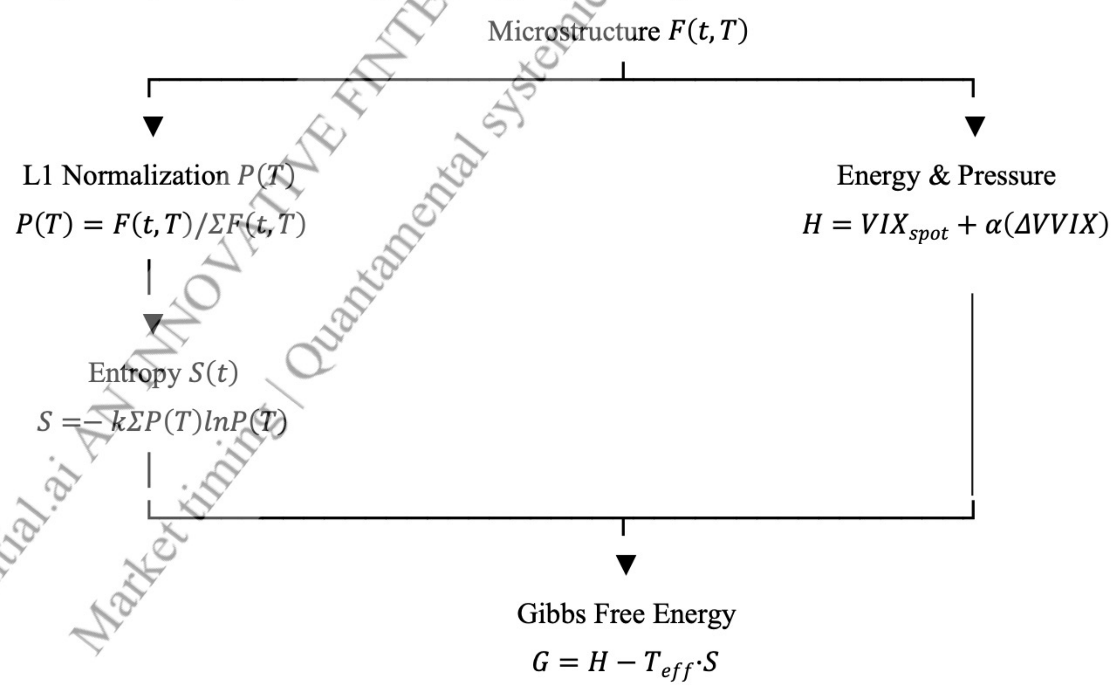

1.3 Effective Temperature, Internal Energy, and Conservation Laws

The system's internal energy $U(t)$ maps directly to $VIX_{spot}(t)$. The First Law of Financial Thermodynamics is expressed as:

$$dU = \delta Q - \delta W$$

where δQ represents exogenous information shocks (macroeconomic news, geopolitical developments) and δW represents market work performed (order flow execution, rebalancing, portfolio hedging). The effective temperature $T_{eff}(t)$ is derived from high-frequency volatility market activity and intensity. In accordance with kinetic gas theory, where collision frequency scales with $\sqrt{T}$, T_{eff} scales proportionally with $VVIX$ $\left(T_{eff} \propto \sqrt{VVIX}\right)$. The Second Law mandates that under idealized shock absorption, $dS \geq \frac{\delta Q}{T_{eff}}$. i.e., that market entropy is non-decreasing under an idealized reading of shock absorption.

1.4 Gibbs Free Energy Potential

Combining $H(t)$, $T_{eff}(t)$, and $S(t)$ yields the Gibbs free energy state function:

$$G(t) = H(t) - T_{eff}(t) \cdot S(t)$$

Classical thermodynamics dictates that G < 0 signifies a spontaneous process. In this financial setting, a negative Gibbs potential indicates that entropy-driven thermal expansion $\left(T_{eff} \cdot S\right)$ exceeds internal energy/enthalpy (H), signifying an unstable state where latent stress is released through panic selling or rapid deleveraging.

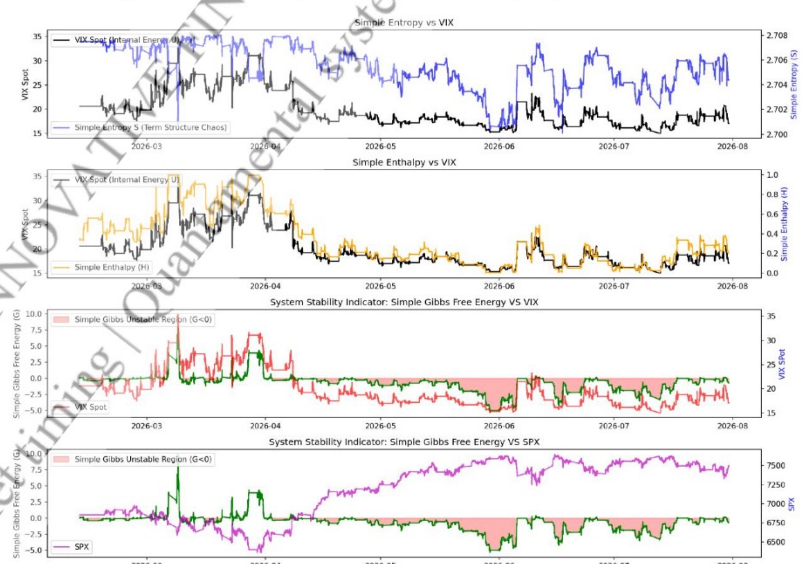

Fig 1. Minutely level illustrations of the non-equilibrium classical thermodynamic state variables from 2026.01-08

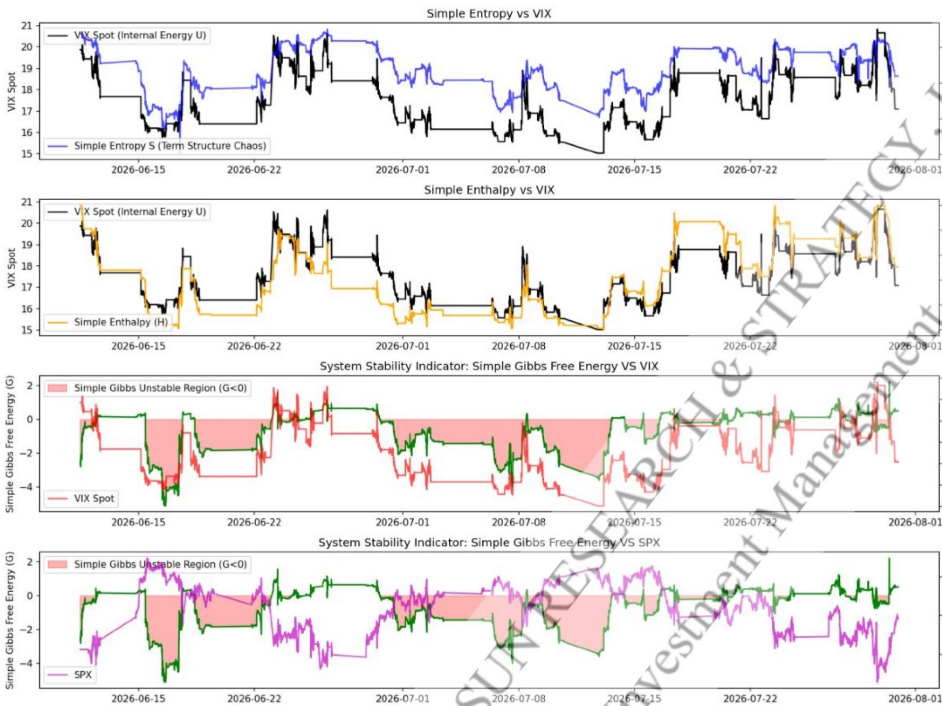

Fig 2. Minutely level illustrations of the non-equilibrium classical thermodynamic state variables from 2026.06-08

2. Kinetic Theory, Boltzmann Transport, and Market Viscosity

2.1 Boltzmann Energy Distribution

The microstructure can be mapped to a classical Boltzmann energy state distribution:

$$P(E) \propto e^{-\beta E}, \quad \text{where } E_i = \ln\left(\frac{F_i}{F_1}\right)$$

where $\beta = \frac{1}{k_B T_{eff}}$ represents inverse market temperature. High goodness-of-fit ($R^2 \approx 0.95 \sim 0.98$) confirms that the microstructure obeys statistical mechanical energy distribution laws during non-crisis regimes, with β parameterizing curve steepness.

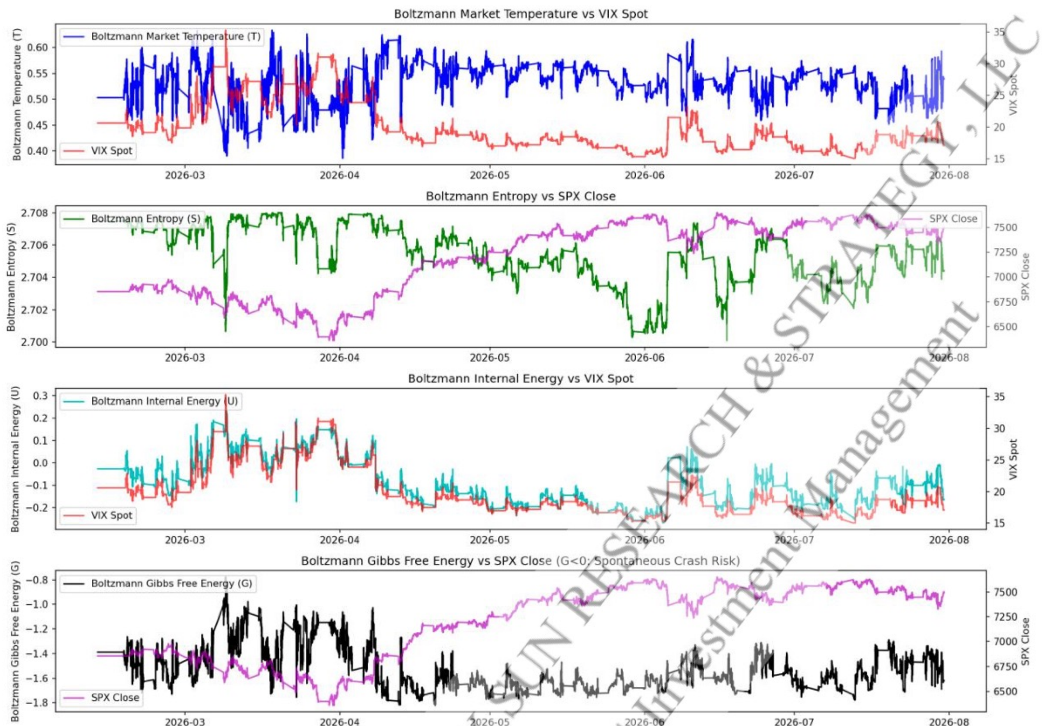

Fig 3. Minutely level illustrations of the Boltzmann Energy Distribution state variables from 2026.02-08

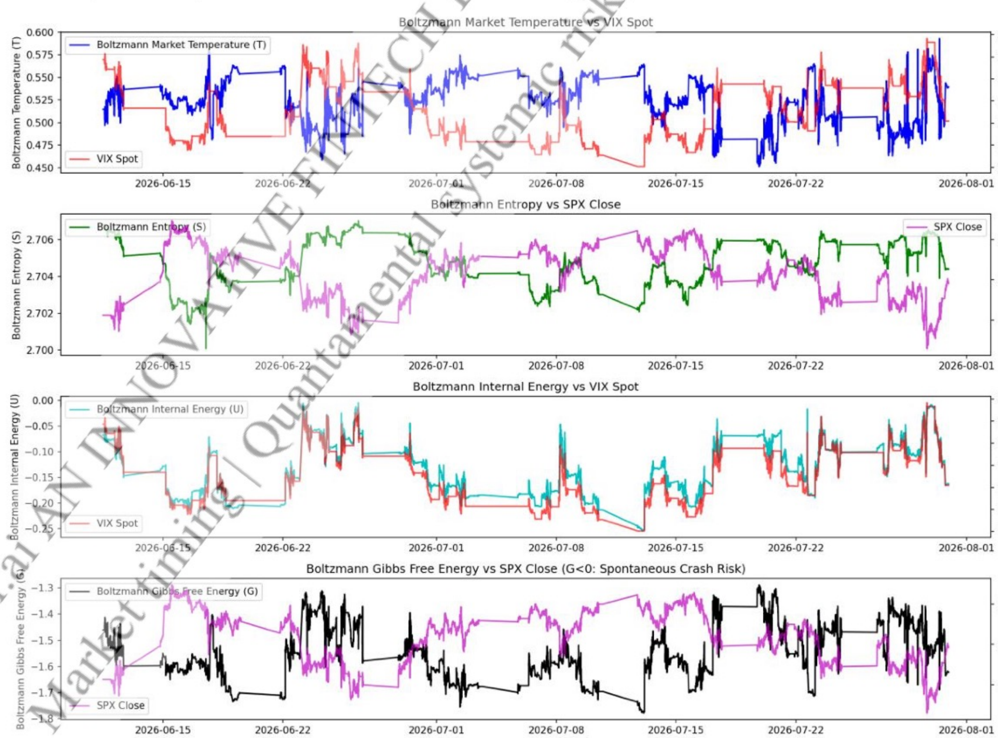

Fig 4. Minutely level illustrations of the Boltzmann Energy Distribution state variables from 2026.06-08

2.2 Collision Dynamics and Relaxation Rates

Drawing from the Boltzmann Transport Equation, market interactions are modeled as discrete particles (orders) undergoing collisions. The collision frequency / relaxation rate $\nu(t)$ defines the velocity at which a disrupted microstructure relaxes back to equilibrium:

$$\nu(t) \propto \sqrt{VVIX(t)}$$

Collision Intensity measures high-frequency pressure from stop-loss triggers and arbitrage execution:

$$\text{Collision Intensity} = \text{Kinetic} \times |T_{VVIX}|$$

where Kinetic is derived from realized volatility proxies (minute-level return variance) and T_{VVIX} reflects temperature changes in the vol-of-vol space.

2.3 Market Viscosity and Liquidity Freeze Mechanisms

To detect "high implied fear, low realized movement" regimes—where quotes widen drastically but trading volume halts—we define Market Viscosity $\eta(t)$ as:

$$\eta(t) = \frac{|T_{VVIX}|}{\text{Kinetic}}$$

High Market Viscosity (η)	Low Market Viscosity (η)
High Implied Stress (|T_VVIX|) Low Realized Movement (Kinetic)	Realized Movement (Kinetic) Dominates Implied Volatility
Liquidity Freeze / Gelling Pre-Halt Market Condition	Smooth Price Discovery Order Flow Absorbable

Table 1. Market Viscosity regimes

When$\eta(t) \rightarrow 1.0$, VVIX-derived thermal pressure dominates realized price motion. Liquidity "gels" or freezes, setting the stage for severe market-gap events. Conversely, low $\eta(t)$ values indicate healthy, fluid risk absorption.

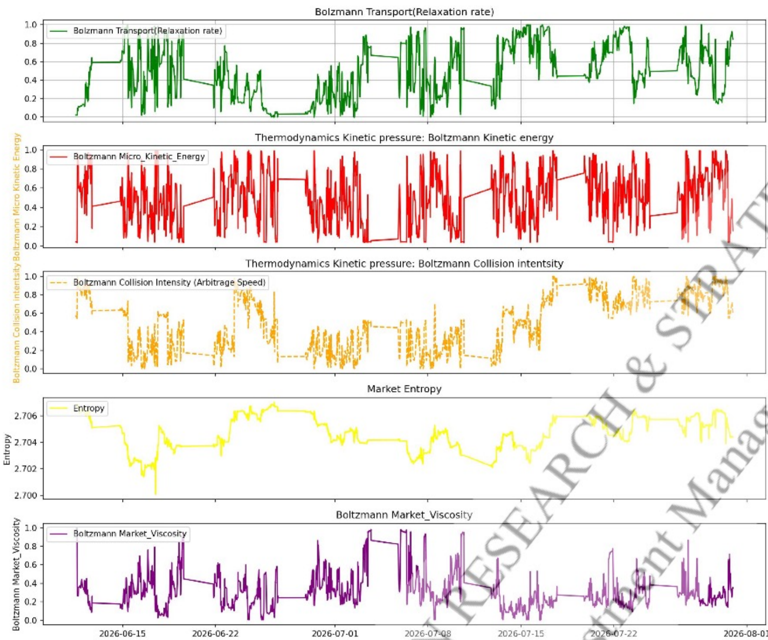

Fig 5. Minutely level illustrations of the Boltzmann Energy Distribution derived Collision Dynamics, Relaxation Rates and Market Viscosity from 2026.06-08

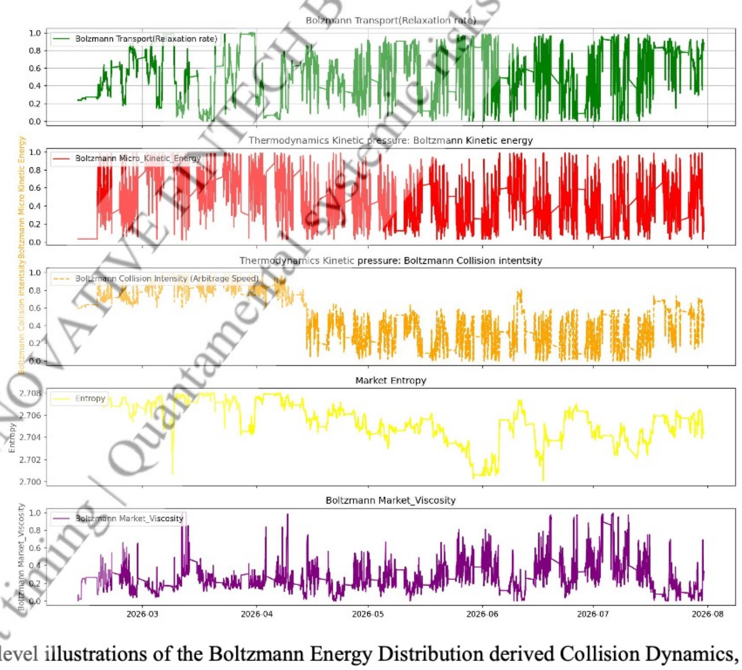

Fig 6. Minutely level illustrations of the Boltzmann Energy Distribution derived Collision Dynamics, Relaxation Rates and Market Viscosity from 2026.02-08

Discussion

3. Empirical Shock Kinematics

A systematic Multi-Regime review of the full spectrum of the system evaluates the empirical performance of $S(t)$, $H(t)$, $U(t)$, and $G(t)$.

3.1 Empirical Baseline of Simple Gibbs Free Energy and Boltzmann Energy Distribution Derived Gibbs Free Energy.

For Simple Gibbs Free Energy, $G_{simple} < 0$ acts as a standalone binary warning flag. For Boltzmann Energy Distribution Derived Gibbs Free Energy, contrary to the initial theoretical hypothesis that $G_{\text{Boltzmann Energy Distribution}} < 0$ acts as a standalone binary warning flag, empirical analysis shows that $G_{\text{Boltzmann Energy Distribution}}(t)$ is persistently negative under ordinary market conditions, operating within a chronic baseline range of -0.5 to -2.0. Informative signals emerge exclusively when $G_{\text{Boltzmann Energy Distribution}}(t)$ deviates significantly from its critical threshold.

3.2 The Shock Kinematics Hypothesis

The key empirical discovery is that the direction and profile of G(t)'s deviation depend directly on the temporal kinematics of the market shock:

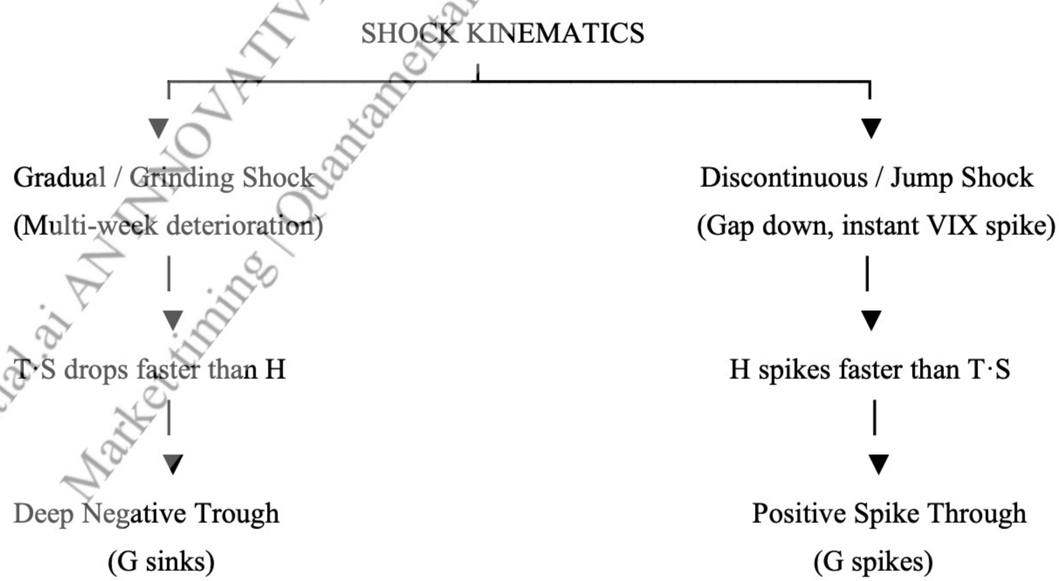

Gradual / Grinding Deteriorations: Multi-week sell-offs allow $T_{eff}(t)$ and $S(t)$ time to adjust continuously alongside H(t). As the front month gradually rises and S(t) drops, the term $T_{eff}(t) \cdot S(t)$ contracts rapidly, pulling G(t) into a deep negative trough (sinking).

Discontinuous / Jump Shocks: Overnight gaps or sudden intraday crashes cause the VVIX pressure term in H(t) to jump instantaneously. Because S(t) and $T_{eff}(t)$ require time-accumulated data to adjust, H(t) far outpaces $T_{eff}(t) \cdot S(t)$ in the short term. This temporal mismatch creates a transient "energy surplus," forcing G(t) to spike sharply positive through the critical threshold.

3.3 Historical Case Studies

Episode	Macro Driver	VIX_{max}	Gibbs Free Energy (G) Response	Kinetic Classification
Sept–Oct 2021	Variant fears, inflation uncertainty	~28	Deep negative trough	Gradual Grinding
Aug–Oct 2023	US Treasury yield spike (10Y \to 5\%)	~22	Smooth negative trough	Gradual Grinding
April 2024	Hawkish CPI inflation repricing	~19	Severe negative trough	Gradual Grinding
August 5, 2024	Yen carry-trade unwind	~65	Extreme positive spike	Discontinuous Jump
April 2025	"Liberation Day" tariff shock	>60	Record positive spike	Discontinuous Jump
Feb–Mar 2026	Tech earnings, hawkish Fed transition, Iran conflict, Opex hedging	~33	Feb: Negative trough ; Mar: Positive spike	Dual Phase (Gradual into Jump)

4. Systemic Risk Diagnostics and Four-Quadrant State Phase Space

4.1 Systemic Risk Diagnostic Procedure

To operationalize the thermodynamic framework, market states are evaluated via a five-step diagnostic process:

Step 1: Sanity Check (U ≈ VIX_spot) ──► Step 2: T_{eff} Amplitude Expansion (Early Warning)

Step 4: G Signal Evaluation ◄── Step 3: S Trajectory Tracking ◄─┘

├── G Critical Threshold Spike ──► Jump Shock Phase Transition

└── G Trough ──► Grinding Stress Accumulation

|

Step 5: Post-Shock Decompression Assessment (G & S Mean Reversion Rate)

1) Pipeline Verification: Ensure $U(t) \approx VIX_{spot}(t)$. Persistent divergence signals pipeline or calculation errors.

2) Early Warning (1–3 Weeks): Monitor the rolling oscillation variance of $T_{eff}(t)$. Expanding T_{eff} variance precedes major market shocks.

3) Regime Classification: Track the trajectory of S(t). A persistent decline indicates steady backwardation build-up. A precipitous drop accompanied by T_{eff} spikes indicates an unfolding jump shock.

4) State Transition Confirmation: Evaluate G(t) relative to baseline. Crossing G critical threshold confirms an active jump shock. Sinking below lower threshold confirms severe grinding stress (cross-verified with SPX price to rule out false positives such as January 2024).

5) Decompression Tracking: Monitor post-shock recovery rates of G(t) and S(t). Rapid mean-reversion signals orderly liquidity restoration. Persistent extreme values signify unresolved structural fragility.

4.2 Four-Quadrant Phase Space

Thermodynamic phase space is categorized into four distinct regimes based on Entropy (S) and Effective Temperature$\left(T_{eff}\right)$:

	Low $\mathbf{T_{eff}}$	High $\mathbf{T_{eff}}$
High **S**	**Liquid State**: Normal Contango	**Gaseous State**: Volatile / Unidirectional Trend
Low **S**	**Solid State**: Frozen / Illiquid	**Overheated Collapse**: Active Discontinuous Panic

➢ Liquid State (High S, Low T_{eff}): Standard, carry-friendly contango curve with high structural entropy and low volatility pressure.

➢ Gaseous State (High S, High T_{eff}): High market activity but well-distributed contract pricing. Represents active price discovery or benign expansion.

➢ Solid State (Low S, Low T_{eff}): Low entropy curve (backwardation) combined with low trading activity. Indicates order book illiquidity and quote gelling.

➢ Overheated Collapse (Low S, High T_{eff}): Extreme backwardation combined with surging vol-of-vol pressure. Associated with positive G(t) spikes, triggering severe liquidation cascades.

5. Main Contributions and Findings

A continuously-valued entropy measure derived from the VIX microstructure rather than a simple spread comparison, allowing regime intensity — not merely regime direction — to be quantified and compared across time and across different regimes that a binary label would treat identically.

A vol-of-vol-augmented energy variable. By constructing H as VIX level plus a VVIX-deviation pressure term, This work represents a novel attempt to encode second-order volatility information (the market's uncertainty about volatility itself) into a single energy-like scalar, rather than treating VVIX as a separate, independently-monitored series.

A single, continuously-valued composite stability potential. Rather than combining VIX level, VIX microstructure, and VVIX through ad hoc weighted scores or independent threshold alarms (as is common in practitioner risk dashboards), this work derives G from a first-principles thermodynamic identity (G = H − TS), giving the composite a specific, falsifiable functional form rather than a discretionary weighting scheme.

A companion liquidity-mechanics layer (Market Viscosity). This work propose a Market Viscosity measure, $\eta(t) = \frac{|T_{VVIX}|}{\text{Kinetic}}$ (VVIX-derived temperature divided by realized-volatility-derived kinetic energy), designed specifically to detect a "high implied fear, low realized movement" divergence — a fluid-mechanics analogy for the pre-halt "gelling" of liquidity in which quotes exist but do not trade. This work regards this as a strong, underexploited candidate mechanism for why G's spikes occur.

We find that G's practically useful signal is not its sign but the direction and context of its deviation from a critical threshold, and that this direction is conditioned on the temporal profile of the underlying shock.

Finding 1 — Internal consistency check. In every reviewed window, the charted "Internal Energy (U)" series overlaps almost exactly with VIX spot, consistent with the first-law identification of U with VIX spot. This is a useful, low-cost sanity check for future chart batches: persistent, non-crisis-period divergence between U and VIX spot should be treated as a data or pipeline defect rather than a market signal.

Finding 2 — Entropy troughs align with panic peaks, with a kinematic caveat. Sharp entropy declines co-occur with SPX local troughs in the large majority of reviewed drawdowns (e.g., the September–October 2021 and December 2025–February 2026 episodes). However, in several fast, discontinuous shocks (August 2024, April 2025), entropy's initial response is more ambiguous — plausibly because a synchronized, whole-curve repricing does not immediately concentrate the distribution the way a slower, front-month-led deterioration does — before entropy ultimately collapses.

Finding 3 — Temperature amplitude expansion as a leading (week-scale) signal, distinct from G. In the weeks preceding the largest shocks in the sample (notably the run-up to the April 2025 episode, visible from mid-March 2025 onward), the variance of T's short-term oscillation — not its level — expands visibly ahead of the event, while G's own extreme excursion is comparatively coincident with, rather than clearly leading, the realized shock. This suggests a two-tier signal structure: T-amplitude for early (week-scale) warning, and G's critical-line breach for event confirmation (day-scale), which we formalize into the risk-assessment checklist.

Finding 4 — The Shock Kinematics Hypothesis. Tabulating G's response across the six episodes examined in detail — the September–October 2021 drawdown, the August–October 2023 rate-driven correction, the April 2024 CPI-driven pullback, the August 5, 2024 yen-carry unwind, the April 2025 tariff shock, and the February–March 2026 drawdowns — we observe a consistent bifurcation. Gradual, multi-week deteriorations (2021 Sept–Oct, 2023 Aug–Oct, April 2024, and the slower leg of the February 2026 decline, which coincided with disappointing mega-cap earnings and a hawkish Federal Reserve leadership transition) are associated with G sinking to a deep negative trough, often without an accompanying spike in absolute VIX level (the April 2024 episode reached VIX only in the high teens). Sharp, discontinuous shocks — the August 5, 2024 unwind, the April 2025 tariff announcement, a single-day December 18, 2024 FOMC reaction, and the March 2026 escalation coinciding with expanded Middle East conflict and options-expiration-related delta-hedging flows — are instead associated with G spiking sharply positive, crossing the G critical threshold by a wide margin. We propose that this reflects a timing mismatch internal to G's own construction: the VVIX-driven pressure term in H can jump within minutes to hours, while the entropy and temperature terms — which depend on the microstructure's relative shape and on activity accumulated over a longer window — adjust with a lag. A sufficiently steep shock therefore transiently produces G Spike ("energy surplus") before entropy and temperature catch up and pull G back down, whereas a sufficiently gradual shock allows T·S to fall in step with (or ahead of) H, pulling G into a deep trough instead. We term this the Shock Kinematics Hypothesis and flag it as this paper's principal original empirical claim.

Finding 5 — A documented false-positive case. One reviewed window (January 2024) shows G plunging to one of the deepest troughs in the entire sample with no corresponding SPX drawdown in the same window. We report this transparently as a caution against using G-trough events in isolation without SPX/VIX confirmation, and future research develop upon this framework can resolve this problem with improved quantum financial system.

Finding 6 — Post-shock decompression rate as a regime-normalization signal. In the cleanest V-shaped recoveries (August 2024, April 2025), G's post-spike decay back toward its chronic baseline was comparatively rapid and accompanied by S's recovery toward its own central range. In the most recent window (April–July 2026), by contrast, T and VIX continued to exhibit elevated, choppy behavior even as G and S largely normalized — a divergence we read as consistent with independent contemporaneous reporting of narrowing market breadth (roughly 56% of S&P 500 constituents above their 200-day moving average even as the index made new highs) and analyst commentary flagging elevated correction risk into the summer of 2026 despite a subdued VIX level. This is offered as a candidate example of the framework identifying "risk cleared at the surface, structural fragility unresolved beneath it," though we emphasize this reading is qualitative.

6. Toward Risk Management and Tactical Applications

The Shock Kinematics Hypothesis has a direct practical implication: a single G-threshold alarm is insufficient, because the economically relevant response depends on which side of the G critical threshold the excursion approaches from, and how fast. A risk system[1-4] built on this framework would benefit from monitoring (i) T's rolling oscillation amplitude as a multi-week early-warning layer, (ii) S's slope as a regime-classification layer (gradual concentration vs. abrupt), and (iii) G's proximity to and crossing of critical threshold as an event-confirmation layer — together with the Market Viscosity construct as a candidate explanatory mechanism linking implied-vol spikes to realized-liquidity freezes.

Conclusion

This work's central contribution is a physically-motivated, continuously-valued alternative to discrete VIX-regime heuristics, built from first principles around the VIX microstructure's entropy, enthalpy, and Gibbs free energy. Our framework represents several important innovations and insights:

First, an information-theoretic reformulation of the contango/backwardation dichotomy, a vol-of-vol-augmented energy state variable, and a single continuously-valued free-energy potential replacing ad hoc VIX-level thresholds. Second, and more substantively, G's economically meaningful signal is not its sign in isolation (i) the amplitude of its deviation from a chronic baseline, and (ii) the direction of its deviation, which empirically bifurcates into deep negative troughs during gradual, grinding deteriorations versus sharp positive spikes through the G critical threshold during discontinuous, gap-type shocks. We term this the Shock Kinematics Hypothesis and illustrate it across six historical episodes, including the August 5, 2024 yen-carry unwind, the April 2025 tariff shock, and the February–March 2026 drawdowns.

This paper presents a novel thermodynamic framework for analyzing the VIX microstructure. The proposed state variables and equations offer new insights into market dynamics and systemic risk. Future research could extend this framework to other financial markets and asset classes.

References:

1. Sun, Huzi. Systematic Integration of Systemic Risk Management and Multi-factor Pricing Dynamics in S&P 500 Price Discovery. *SSRN,* **2026**. http://dx.doi.org/10.2139/ssrn.7223479.

2. Huzi Sun. State of the Art Macro Risk Controlled Risk Parity Model for Macro Multi-Strategy Funds. **2026**, PREPRINT.

3. A global asset allocation system based on a macro alternative multi-factor rating model. *Patent number: CN202511140743.3A*

4. An all-weather global asset allocation system based on macro alternative multi-factor rating models. *Global PCT Patent, Application No. PCT/CN2026/112498*

5. Rubina Zadourian. Model-based and empirical analyses of stochastic fluctuations in economy and finance. *arXiv,* **2024**, PREPRINT

Competing interests: †Core technical implementation protected by Chinese Patent Application No.CN202511140743.3A (Filed: 2025-08-14) and Patent Cooperation Treaty (PCT) international patent application No. PCT/CN2026/112498 (Filed: 2026-07-22). Full patent documentation available via CNIPA/WIPO.

Data, code, and materials availability: All data, code, and materials used in the analysis are available upon requests and signing the materials transfer agreements (MTAs) for purposes of reproducing or extending the analysis.

Declaration of Funding: This work was conducted independently and is self-supported by the author through Sun Research & Strategy, LLC. The author is the founder and owner of Sun Research & Strategy, LLC. The author declares that the company may have a financial interest in the subject matter, patents, or findings discussed in this article.